water

MDPI

Article

Limnological Characteristics and Relationships with Primary Productivity in Two High Andean Hydroelectric Reservoirs in Ecuador

Gonzalo Sotomayor [1,*], Andrés Alvarado [2,3], Jorge Romero [4], Carlos López [5], Marta Aguilar [6], Marie Anne Eurie Forio [7] and Peter L. M. Goethals [7]

[1] Centro de Investigaciones Aplicadas y Mejoramiento de la Productividad Empresarial (SAPIENS), Facultad de Ingeniería, Universidad Hemisferios, Paseo de la Universidad, 300, Quito 170147, Ecuador
[2] Departamento de Recursos Hídricos y Ciencias Ambientales, Universidad de Cuenca, Av. 12 de abril s/n, Cuenca 010150, Ecuador; andres.alvarado@ucuenca.edu.ec
[3] Facultad de Ingeniería, Universidad de Cuenca, Av. 12 de abril s/n, Cuenca 010150, Ecuador
[4] Instituto de Estudios del Régimen Seccional del Ecuador (IERSE), Facultad de Ciencia y Tecnología, Universidad del Azuay, Av. 24 de Mayo 7-77, Cuenca 010150, Ecuador; jaromero@uazuay.edu.ec
[5] Escuela Superior Politécnica del Litoral (ESPOL), Centro de Agua y Desarrollo Sustentable, Guayaquil 2019, Ecuador; cllopez@espol.edu.ec
[6] Unidad de Gestión Socioambiental, Empresa Electro Generadora del Austro (Elecaustro S. A.), Av. 12 de abril s/n, Cuenca 010150, Ecuador; marta.aguilar@elecaustro.gob.ec
[7] Department of Animal Sciences and Aquatic Ecology, Faculty of Bioscience Engineering, Ghent University, Coupure Links 653, 9000 Ghent, Belgium; marie.forio@ugent.be (M.A.E.F.); peter.goethals@ugent.be (P.L.M.G.)
* Correspondence: gonzalo.sotomayor-v@uhemisferios.edu.ec

Abstract: Studies on limnology are essential to reservoir management; nevertheless, few are known about the limnological features of the Andean reservoirs in Ecuador. To overcome this limitation in the information, from December 2018 to December 2019, the limnological characteristics of El Labrado and Chanlud reservoirs in the Machángara river basin (Ecuador south) were examined. Using the light/dark bottles technique, the primary productivity (PP) of phytoplankton was studied in conjunction with (1) vertical profiles of oxygen concentrations, water temperature, nitrogen, phosphorus, alkalinity, and heterotrophic bacteria; (2) Secchi disk transparency; and (3) meteorological factors such as wind force, precipitation, and water level. Data indicate that both reservoirs are polymictic, with alkaline waters, low nutrients, and low PP rates. Despite this, a principal component analysis revealed that Chanlud exhibits higher nitrogen, alkalinity, heterotrophic bacteria, and PP values. In two approaches through multiple linear regression analysis, each per reservoir, the PP was explained mainly by water temperature, depth, light, heterotrophic bacteria, and meteorological parameters. The low concentrations of nutrients and the low residency time explain the low PP values. Likewise, the altitudinal factor (i.e., both reservoirs are 3400 m above sea level) and the low human perturbations in surrounding reservoir zones play a crucial role in explaining their poor PP. Notwithstanding the low metabolic rates, clear seasonal trends were observed in both reservoirs; the lowest PP rates occurred during the cold season. To our knowledge, this is the first limnological study of high Andean reservoirs in Ecuador. These findings should be part of Andean reservoir management protocols, contributing significantly to local conservation efforts. Additionally, they could be extrapolated as a frame of reference to similar eco-hydrological systems.

Keywords: limnological features; primary productivity; high Andean reservoirs

check for updates

Citation: Sotomayor, G.; Alvarado, A.; Romero, J.; López, C.; Aguilar, M.; Forio, M.A.E.; Goethals, P.L.M. Limnological Characteristics and Relationships with Primary Productivity in Two High Andean Hydroelectric Reservoirs in Ecuador. *Water* **2024**, *16*, 2012. https://doi.org/10.3390/w16142012

Academic Editors: Dubravka Čerba, Maja Raković, Djuradj Milošević and Filip Stevic

Received: 5 June 2024
Revised: 6 July 2024
Accepted: 9 July 2024
Published: 16 July 2024

Copyright: © 2024 by the authors. Licensee MDPI, Basel, Switzerland. This article is an open access article distributed under the terms and conditions of the Creative Commons Attribution (CC BY) license (https://creativecommons.org/licenses/by/4.0/).

1. Introduction

Reservoir construction is one of the most remarkable human activities in modifying freshwater ecosystems. It is a widespread practice worldwide that involves utilizing rivers

by building a series of reservoirs [1]. In this sense, dams are infrastructures commonly related to reservoirs. Dams/reservoirs are primarily designed for hydroelectric power generation [2] and other uses such as irrigation, flood control, water supply, improved navigation, fish culture, recreation, or some combination. However, damming water courses exerts negative effects; dams/reservoirs can adversely affect the structure and functioning of aquatic ecosystems [3], downstream [4] and in situ. Several problems arise in situ with the slowing down of running water added to inadequate land use management of the surrounding areas of the reservoirs; the best known are eutrophication [5,6], the loss of biodiversity [7], and greenhouse gas emissions [8], among others.

Limnology is a comprehensive science that deals with water systems and the surrounding land. It considers physical, chemical, geological, and biological features to provide conceptual models of freshwater ecosystems and fundamental information needed to determine causes and potential solutions to environmental stresses [9]. Therefore, limnological characterization is a key tool for designing reservoirs' conservation and management plans [10,11] in response to, for example, ongoing climate change [12] or catchment disturbances [13]. Particularly in a region such as the Andes, whose ranges extend along western South America, from south Venezuela to Tierra del Fuego, with irregular topology [14], where multiple stressors and increasing water demands impose unprecedented stress on freshwater ecosystems, the inclusion of a limnological framework of research is crucial. The ability to assess the response of Andean freshwaters to anthropogenic stressors requires knowledge of baseline limnological conditions [15]. However, with a few notable exceptions, limnological surveys in the tropical Andes reservoirs are rare [16–21]. Except in Brazil [22–26], knowledge about neotropical reservoirs is extremely limited, and this trend is more significant for the high Andean region. In Ecuador, where many reservoirs have been implemented during the last two decades, limnological studies of these artificial ecosystems are non-existent, and no information is available. Up to now, only water quality has been analyzed for Ecuadorian reservoirs from the point of view of compliance with the limits required by Ecuadorian environmental legislation (gray literature), and most limnological research on lentic ecosystems is focused only on natural lakes [27]. Thus, although the overall principles and controlling factors that govern lakes and reservoirs are the same, the premise to consider is that reservoirs were made artificially, and their dynamics are not controlled naturally, i.e., they exhibit many differences relative to natural lakes; consequently, specific studies must be performed to evaluate and characterize reservoirs [28].

Our paper describes, for the first time, the limnological features of two adjacent high hydroelectric Andean reservoirs (i.e., Chanlud and El Labrado) in austral Ecuadorian Andes and their seasonal variations. This study aims to add to the understanding of the limnological characteristics of tropical Andean reservoirs and contribute to management efforts. The results will also form an important baseline for information on assessed reservoirs. We estimate the primary production of both reservoirs concerning selected environmental parameters. We addressed three research questions/goals: (i) What are the differences in limnological features between reservoirs? (ii) What are the main driving factors for primary productivity in the studied reservoirs? Furthermore, (iii) we aimed to study the seasonal limnological variability of the assessed reservoirs.

2. Materials and Methods

2.1. Study Area

The Andes in Ecuador are divided into eastern and western ranges. The second divides the Pacific and Atlantic slopes [29]. The studied reservoirs, Chanlud and El Labrado, are located on the Atlantic slopes in the upper area of the Machángara river basin, which belongs to the Paute river basin (Figure 1). The total area of the Machángara catchment is 323.55 km^2, and the altitude range is 2424 to 4424 m above sea level (m a.s.l.); that is, this is a typical hydrologic system of the Andean páramo ecosystem of South America [30]. The average annual precipitation varies between 877 mm and 363 mm per year, while the

average annual temperature fluctuates between 16.0 °C and 9.0 °C in the lower and upper areas, respectively [31]. Two seasons are present during the year: a season of precipitation from the middle of February to the beginning of July and a dry season during the rest of the year. The average flow of the Machángara river measured from 1964 to 2010 was 8.4 m^3 s^{-1}, and this river is used for domestic and industrial purposes, agricultural irrigation, and hydropower generation. Currently, 60% of Cuenca's drinking water (Ecuador's third largest city) comes from the Machángara hydrological system.

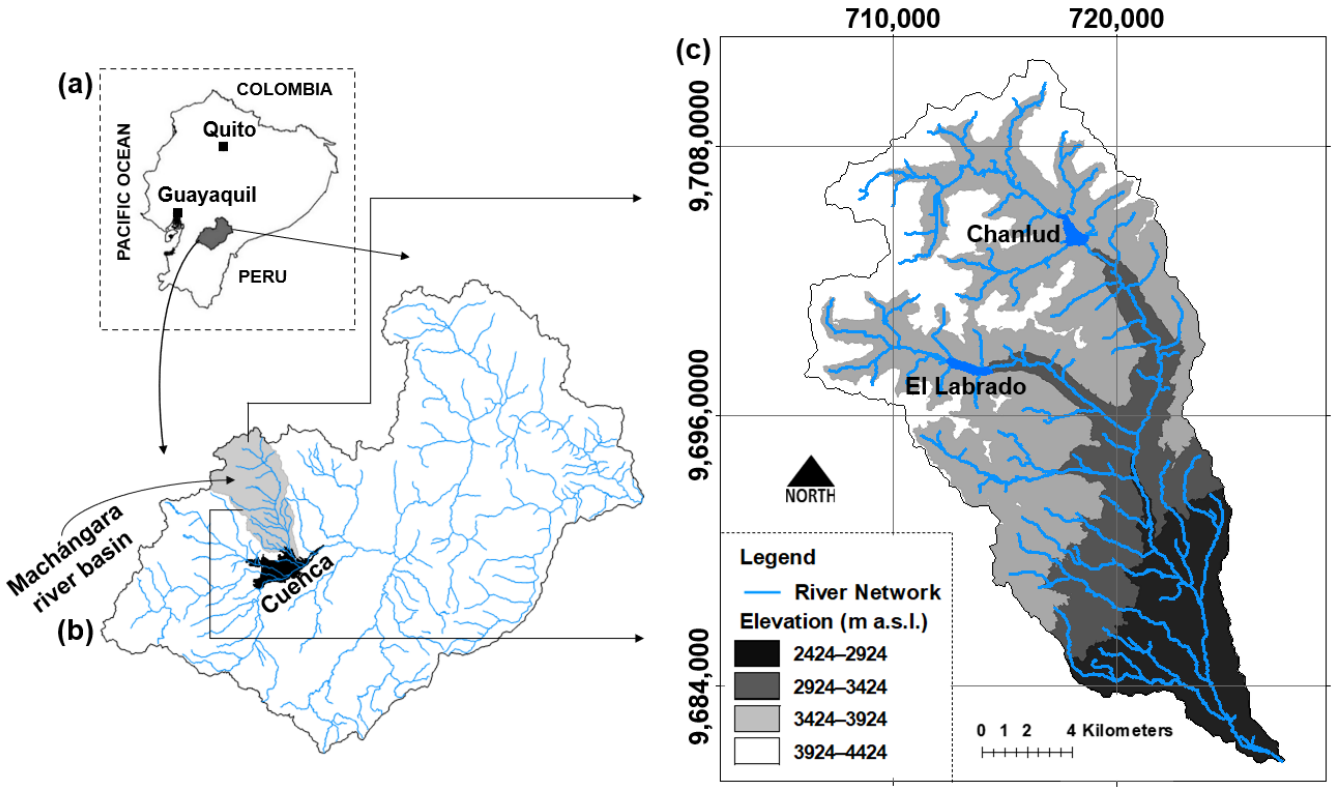


Figure 1. (**a**) Location of the Paute river basin in continental Ecuador and its largest city (Cuenca); (**b**) location of the Machángara river basin in the Paute river basin and (**c**) elevation distribution and the river network in the Machángara river basin. Coordinate system: WGS84 UTM 17S; coordinate units: meters.

Regarding the reservoirs Chanlud and El Labrado, the former is in the Machángara Alto River sub-basin, and the latter is in the Chulco river sub-basin. Both reservoirs form the Machángara River Hydroelectric Complex. The Chanlud reservoir became operational in 1992 and is located at 3464 m a.s.l. (at their centroid point); it has a maximum depth of 40 m, a storage capacity of 17 hm^3, and a regulated discharge of about 4.8 m^3 s^{-1}. The reservoir area is ~0.69 km^2, and its shoreline is 5.6 km. El Labrado reservoir became operational in 1972 and is located at 3418 m a.s.l. (at their centroid point); it has a maximum depth of 14 m, a storage capacity of 6.15 hm^3, and a regulated discharge of about 2.4 m^3 s^{-1}. The reservoir area is ~0.58 km^2, and its shoreline is 5.1 km [32]. In 1985, the national environmental authorities declared the upper area of the watershed of Machángara a protected forest (i.e., Machángara–Tomebamba protected area), so human activities such as agriculture, etc., were restricted in the surrounding areas of both studied reservoirs (for Chanlud, 0.3% of their contributing basin is anthropized, and for El Labrado, the percentage is 0.5%). However, the middle and lower zones of the Machángara watershed continued to deteriorate [33].

2.2. Sampling Design

For both reservoirs, sampling campaigns from December 2018 to October 2019, and December 2019, were performed in their deepest part (previously determined through bathymetry) between 8.30 and 16.30 h, with a spatial replicability of one site per reservoir. Vertical samples were taken every 5 and 3 m from surface to bottom in Chanlud and El Labrado, respectively, using a Van Dorn sampler (2L). The different intervals of vertical sample design were due to the significant dissimilarities in depth and their variability for both reservoirs. For Chanlud, the range of depth was 30.7–39.5 m, while for El Labrado, it was 8.4–14.1 m. Vertical sampling for El Labrado every 5 m was assumed to have a low number of samples, which would have negative implications for integrated analysis based on the scalar vector of depth. Therefore, vertical sampling was performed for this reservoir every 3 m of depth. Due to the water level variability of both reservoirs, their depths were first measured per visit using sonar (Speedtech® depth-mate portable sounder). Thus, the number of vertical samples per reservoir was established as a function of depth during the start of the field visit. For each water sample at each depth, measurements of alkalinity (mg L^{-1} of $CaCO_3$), orthophosphate (mg L^{-1} of $PO_4{}^{3-}$), nitrite (mg L^{-1} of $NO_2{}^{-}$-N), nitrate (mg L^{-1} of $NO_3{}^{-}$-N), heterotrophic bacteria (bacteria 100^{-1} mL^{-1}), and ammonium (mg L^{-1} of $NH_4{}^{+}$-N) were performed. Orthophosphate, nitrite, nitrate, and ammonium were obtained using a modular system for performing continuous flow analysis (OI Analytical—Flow Solution® FS 3100), with the detection limits being 0.001, 0.0005, 0.0005, and 0.0005 mg L^{-1}, respectively. Alkalinity was determined by a titrimetric approach, SM 2320 B method [34], with a detection limit of 8 mg L^{-1}. Heterotrophic bacteria were estimated by the spread plate method, in which the water sample was mixed for 5 min at low speed before serial dilution. Samples were spread in duplicate on a pre-cooled agar plate consisting of a glucose–nitrogen minimal medium with a 0.2% *w*/*v* casamino acids supplement. Plates were incubated at 22 °C for 3, 5, and 7 days and at 37 °C for 1, 3, and 5 days [35].

Vertical profiles of water temperature (°C) and dissolved oxygen (mg L^{-1} of O_2) were performed using EXO2 sonde [36] at one-second intervals. Light penetration in the water column was determined with a standard Secchi disk (Z_{sd}) (25 cm in diameter) in meters. The depth (m) of the euphotic zone (Z_{eu}) was assumed equivalent to 1% of the surface light level and was estimated by multiplying the Secchi-disk depth (Z_{sd}) by a factor of 2.7 [37,38]. The light vertical extinction coefficient (E_v) was calculated using this equation: $E_v{}^n \times Z_{sd}$ = constant, where n = 0.84, and the "constant" is 1.54 [39,40]. Likewise, an integrated water sample from the Z_{eu} was taken to determine chlorophyll-*a* concentration (μg L^{-1}) in the laboratory through spectrophotometric analyses of acetone extracts [41], with a detection limit of 0.023 μg L^{-1}.

In this context, photosynthesis and phytoplankton are the prime components of aquatic primary production, and chlorophyll-*a* is a fundamental indicator of phytoplankton abundance [42]. Herein, primary productivity (PP) was obtained by measuring oxygen concentrations in dark and clear bottles incubated in situ at various depths (i.e., every 5 and 3 m for the Chanlud and El Labrado reservoirs, respectively) throughout the water column, using a line of supports placed on an anchor located in the deepest part of each reservoir. Thus, the number of incubation levels was established as a function of the depth for each reservoir per visit. Each bottle was filled with water from the corresponding depth. Lightproof bags were used to store dark bottles wrapped in aluminum foil. A wood wire frame with an attached rope held the bottles vertically at 25 cm to prevent self-shading. Before placing the bottles on the supports and starting the incubation, the initial dissolved oxygen concentration (initial O_2) in each was measured using a HANNA oximeter (model HI 9146). Another measure of oxygen was performed after the incubation (final O_2). Calculations of gross primary production (GPP) and net primary production (NPP) and respiration (R) rates were based on the changes in the oxygen content in the light and dark bottles. The initial O_2 concentration (c1) could be expected to decrease to a lower value by R in dark bottles (c2) and increase to a higher concentration (c3) in clear

bottles, according to the difference between photosynthetic production and respiration [43]. The difference (c1 − c2) represents R activity per unit volume during the incubation time interval (Δt) (for both bottles, the average Δt was 5:56 h, ± 0:52 standard deviation). The difference (c3 − c1) is equal to the NPP, and the sum (c3 − c1) + (c1 − c2) = (c3 − c2) corresponds to the GPP [40]. To obtain the PP (i.e., GPP + NPP) and R rates per area and time units (mg C m^{-2} d^{-1}) for each sampling month, vertical integrations were performed through the trapezoidal method [44–46]. Thus, since R, NPP, and GPP are vectors, the method calculated the integrated function for them concerning the scalar space specified by the depth (i.e., 0, 5, 10. . ., and 0, 3, 6. . ., m for the Chanlud and El Labrado reservoirs, respectively). The trapezoidal rule is a method that approximates integration over an interval by breaking the area under the curve into trapezoids with more easily comparable areas [47]. Herein, the trapezoidal vertical integrations were carried out using the "trapz" function of MATLAB® [48]. For the PP, the integrations were calculated on the Z_{eu}, and the day length was assumed to be 12 h. The integral function for R was calculated for the entire water column over 24 h, assuming that the R rate at night was the same as during the day [39,49].

Finally, meteorological parameters such as precipitation (mm) and wind force (m s^{-1}) were considered. These variables were obtained using two meteorological stations located in the proximity of each dam wall (for Chanlud, N −2°40′45″ E −79°2′1″ and for El Labrado, N −2°43′44″ E −79°4′22″). Sub-daily data were recorded from the meteorological stations during the study period, and they were aggregated into daily datasets and finally to a monthly frequency (i.e., accumulated for precipitation and averaged for wind force).

2.3. Data Analysis

Considering the varying number of records for each parameter in the two reservoirs (e.g., numerous monthly records for water temperature versus only one per month for primary productivity), the data analysis relied on a single monthly value for each parameter and reservoir. An aggregate process was carried out for the parameters with multiple values based on central tendency measures. To perform this, the normality of each dataset per parameter and month was checked using the Shapiro–Wilk (S-W) test [50], considering a 95% confidence level. For a particular parameter, if the S-W test suggested normality, their mean value was used for aggregating; otherwise, the median was used [51,52]. The S-W tests were performed through the shapiro.test() function in the R environment [53]. As a result, a matrix/database (X1) was developed for n_{sp} = 2 sampling points, one per reservoir, n_{rep} = 24 sampling replicates, 12 monthly records per reservoir that overall contained n_{var} = 18 variables, resulting in a total of n_{obs} = 432 observations ($n_{obs} = n_{var} \times n_{rep}$), which are represented by $X1_{i,j}$, with i = 1, 2, . . ., n_{var} and j = 1, 2, . . ., n_{rep}. Once the matrix X1 was organized, a Pearson correlation analysis was performed for their n_{var} to exclude redundant information characterized by a positive or negative correlation magnitude above 0.75 [54]. This was achieved to minimize multicollinearity issues. Pearson correlation analysis was performed using the R environment's cor() function [53]. Likewise, parameters with weak chemical signals were excluded from the data analysis. After the matrix was stripped of redundant and weak signals (i.e., X2), a range scaling process [55] was used to standardize its associated distribution ($X2_z$). Then, a principal component analysis was performed for $X2_z$.

2.3.1. Principal Component Analysis (PCA)

The PCA is an ordination method where the original data matrix (herein $X2_z$) is reduced to parts A_L (loadings) and U_S (scores). A_L indicates how much an original variable is "loaded into" a principal component (PC), and U_S are the coordinates of one replicate in the new system [56,57]. Linear combinations of A_L and U_S reproduce the matrix $X2_z$ as new synthetic variables that are non-correlated between them, representing a certain quantity of variables of the $X2_z$ and explaining their variance [58]. A critical prior task of a PCA is selecting an optimal number of PCs [59]. Herein, the Average Eigenvalue Criterion

(AEC) was used for this purpose through the Venetian blinds cross-validation method. AEC is based on eigenvalues and only accepts components with an eigenvalue larger than the average eigenvalue as significant [59]. The Venetian blinds cross-validation method is based on splits of observed data [60–62]. In this research, the n_{rep} was split into five splits [63] for cross-validation (i.e., four groups for model training and the fifth group for validation). To perform the ordination PCA process, a quantitative response vector was loaded to $X2_z$, corresponding to n_{sp} (i.e., 1, 2 reservoirs) to assess the potential differences between studied reservoirs. The response vector does not affect PCA calculation, but it allows for a visual differentiation of samples/replicates during interpretation. Within this framework, through A_L, PCA identifies the most informative original variables that explain the differences between both reservoirs. For this purpose, the "cut-off rule" criterion was applied [64], which regards $|\text{loadings}| > 0.25$ as being significant [65]. Furthermore, Fisher's least significant difference (LSD) test was used to calculate/visualize intervals around the means of the most significant variables (i.e., $|\text{loadings}| > 0.25$). These intervals were constructed in such a way that if two means were the same, their intervals would overlap 95.0% of the time; on the contrary, any pair of intervals that did not overlap vertically corresponded to a pair of means that had a statistically significant difference [66]. The PCA was implemented with MATLAB® using the PCA toolbox version 1.3 [59], and the LSD test was calculated using the LSD.test() function in the R® package "agricolae" [67].

2.3.2. Multiple Linear Regression Analysis (MLRA)

Finally, to identify the informative parameters that explain the variability of the PP (GPP + NPP), using $X2_z$, two multiple linear regression analyses (MLRA) were performed, each one per reservoir (i.e., $MLRA_{Ch}$ and $MLRA_L$). In each MLRA, the PP was the dependent variable, and the rest of parameters were independent ones [68]. Backward stepwise selection (BSS) (i.e., a stepwise selection method) was applied to identify the independent variables with statistic effects on the dependent variable. Beginning with a model that includes all variables, the BSS removes variables one at a time if they are not statistically significant (i.e., variables are removed from the model at a given step if their *p* values are greater than the P-to-Remove value, herein fixed as 0.05) [69]. Thus, the most informative explanatory variables to explain the variability of PP were identified at the end of the process [70]. To evaluate each MLRA, the Adjusted R-squared (Adj—R^2) statistic was used. Also, the Durbin–Watson (DW) [71] statistic test was implemented for the residual and serial correlation assessment. Finally, an analysis of variance was performed for each MLRA. Of particular interest were the F-tests and their associated *p*-values, which test the statistical significance of the fitted model. A small *p* value (less than 0.05) indicated a significant relationship between PP and the independent variables. Both MLRAs were performed using the lm() function in the R environment [53].

3. Results

After Pearson correlation analysis, eleven variables were chosen for the planned statistical protocol: dissolved oxygen (O_2), water temperature (WT), nitrate (NO_3^--N), alkalinity ($CaCO_3$), heterotrophic bacteria (HB), wind force (WF), Secchi disk (Z_{sd}), maximum depth (D_{max}), primary productivity (PP), chlorophyll-*a* (Chl) and precipitation. The excluded variables were the euphotic zone (Z_{eu}), light vertical extinction coefficient (E_v), respiration (R), and gross and net primary productivity (GPP and NPP, respectively). Orthophosphates (PO_4^3), nitrites (NO_2^--N), and ammonium (NH_4^+-N) were not detected in both reservoirs; only trace values were registered for them. Therefore, these parameters were not considered for the statistical analysis. A summary of assessment parameters for both reservoirs is given in Table 1 (for most cases, henceforth, the mean is termed $\bar{x}$).

Table 1. Summary of assessment parameters for both reservoirs. The first ten columns show the means ± standard deviations. For the last nine columns, there are unique values because of the nature of the variables. Values highlighted in gray come from datasets with non-normal distributions for which the median instead of the mean value was used for data analysis. WT = water temperature, O_2 = dissolved oxygen, $CaCO_3$ = alkalinity, NO_3^--N = nitrate, NO_2^--N = nitrite, NH_4^+-N = ammonium, PO_4^{3-} = orthophosphate, HB = heterotrophic bacteria, WF = wind force, PPt = precipitation, E_v = light vertical extinction coefficient, D_{max} = maximum depth, Z_{sd} = Secchi disk, Z_{eu} = euphotic zone, Chl = chlorophyll-*α*, GPP = gross primary productivity, NPP = net primary productivity, PP = primary productivity, and R = respiration.

		WT (°C)	O_2	$CaCO_3$	NO_3^--N (mg L^{-1})	NO_2^--N	NH_4^+-N	PO_4^{3-}	HB (bac. 100^{-1} ml^{-1})	WF (m s^{-1})	PPt (mm)	E_v (−)	D_{max}	Z_{sd} (m)	Z_{eu}	Chl (μg L^{-1})	GPP	NPP (mg C m^{-2} d^{-1})	PP	R
Chanlud reservoir	dec-18	11.92 ± 0.47	6.09 ± 0.28	44.38 ± 2.17	0.11 ± 0.16	0.01 ± 0.01	0.03 ± 0.02	0.01 ± 0.00	3.43 ± 2.37	0.84 ± 0.13	0.12 ± 0.19	17.74	32.70	6.57	17.74	1.60	11.67	8.14	19.81	9.73
	jan-19	11.80 ± 0.70	6.26 ± 0.20	48.97 ± 17.66	0.04 ± 0.02	0.01 ± 0.00	0.04 ± 0.02	0.01 ± 0.01	9.67 ± 8.59	0.90 ± 0.21	0.16 ± 0.21	16.07	30.70	5.95	16.07	6.24	10.25	9.97	20.22	0.56
	feb-19	11.91 ± 0.87	6.61 ± 0.21	42.12 ± 4.9	0.10 ± 0.16	0.03 ± 0.07	0.05 ± 0.01	0.00 ± 0.00	0.50 ± 1.07	0.68 ± 0.20	0.23 ± 0.26	12.96	35.10	4.80	12.96	0.80	4.95	3.17	8.12	3.57
	mar-19	11.49 ± 0.62	6.19 ± 0.35	42.26 ± 3.24	0.02 ± 0.01	0.00 ± 0.00	0.06 ± 0.01	0.04 ± 0.03	1.38 ± 2.50	0.61 ± 0.15	0.24 ± 0.32	12.83	38.10	4.75	12.83	0.53	12.38	10.29	22.67	6.99
	apr-19	11.21 ± 0.30	5.80 ± 0.72	42.39 ± 2.29	0.01 ± 0.01	0.06 ± 0.03	0.04 ± 0.02	0.01 ± 0.01	3.50 ± 5.81	0.51 ± 0.20	0.16 ± 0.22	11.29	39.10	4.18	11.29	0.53	13.65	8.02	21.67	12.75
	may-19	11.15 ± 0.62	6.06 ± 0.43	39.83 ± 3.06	0.03 ± 0.01	0.02 ± 0.01	0.04 ± 0.01	0.03 ± 0.00	4.29 ± 7.93	0.64 ± 0.22	0.17 ± 0.20	14.93	38.10	5.53	14.93	2.67	10.47	6.81	17.28	9.37
	jun-19	8.97 ± 0.46	7.80 ± 0.17	35.28 ± 2.62	0.07 ± 0.05	0.01 ± 0.00	0.05 ± 0.01	0.00 ± 0.00	42.50 ± 45.53	0.85 ± 0.32	0.26 ± 0.28	12.47	38.40	4.62	12.47	2.41	8.06	4.32	12.38	8.13
	jul-19	8.97 ± 0.38	7.77 ± 0.16	33.63 ± 1.70	0.03 ± 0.02	0.01 ± 0.00	0.05 ± 0.01	0.00 ± 0.00	63.86 ± 94.36	0.84 ± 0.20	0.19 ± 0.23	11.53	38.50	4.27	11.53	1.17	4.12	3.85	7.97	0.53
	aug-19	7.96 ± 0.31	7.12 ± 0.10	37.03 ± 2.62	3.51 ± 2.79	0.02 ± 0.02	0.07 ± 0.02	0.01 ± 0.00	29.86 ± 18.22	1.00 ± 0.25	0.16 ± 0.22	12.64	38.75	4.68	12.64	0.53	6.64	5.44	12.08	2.74
	sep-19	9.14 ± 1.08	7.17 ± 0.11	40.58 ± 5.07	4.24 ± 2.81	0.01 ± 0.00	0.06 ± 0.01	0.01 ± 0.00	76.57 ± 34.80	0.84 ± 0.08	0.09 ± 0.14	16.36	34.50	6.06	16.36	1.34	8.75	7.41	16.16	2.72
	oct-19	9.87 ± 0.84	7.11 ± 0.29	40.91 ± 1.16	0.06 ± 0.06	0.01 ± 0.00	0.05 ± 0.01	0.01 ± 0.00	13.29 ± 11.25	0.75 ± 0.16	0.23 ± 0.26	13.64	39.50	5.05	13.64	0.41	8.85	5.64	14.49	9.17
	dec-19	11.87 ± 0.42	6.40 ± 0.52	39.51 ± 2.32	0.02 ± 0.01	0.01 ± 0.00	0.03 ± 0.01	0.00 ± 0.00	20.71 ± 19.20	0.87 ± 0.17	0.19 ± 0.21	14.90	38.00	5.52	14.90	1.84	19.45	12.96	32.41	22.44
El Labrado reservoir	dec-18	11.92 ± 0.14	6.48 ± 0.01	29.78 ± 3.10	0.03 ± 0.00	0.00 ± 0.00	0.04 ± 0.03	0.02 ± 0.02	3.67 ± 2.08	0.84 ± 0.25	0.10 ± 0.11	17.82	8.40	6.60	17.82	1.34	2.04	1.38	3.42	1.36
	jan-19	12.02 ± 0.28	6.52 ± 0.09	29.23 ± 1.25	0.04 ± 0.03	0.01 ± 0.01	0.03 ± 0.00	0.01 ± 0.01	2.25 ± 2.22	0.90 ± 0.29	0.14 ± 0.18	14.31	10.10	5.30	14.31	2.67	1.90	1.72	3.62	0.39
	feb-19	12.23 ± 0.41	6.60 ± 0.07	28.58 ± 1.81	0.11 ± 0.04	0.00 ± 0.00	0.03 ± 0.00	0.0 ± 0.00	6.20 ± 5.31	0.68 ± 0.28	0.21 ± 0.22	16.47	14.10	6.10	16.47	0.36	2.05	1.32	3.37	1.46
	mar-19	12.93 ± 0.68	6.52 ± 0.16	28.19 ± 2.69	0.03 ± 0.02	0.00 ± 0.00	0.05 ± 0.02	0.03 ± 0.03	0.00 ± 0.00	0.61 ± 0.26	0.21 ± 0.24	17.36	10.80	6.43	17.36	0.27	3.46	1.88	5.34	3.20
	apr-19	12.90 ± 0.10	6.76 ± 0.06	29.70 ± 1.08	0.02 ± 0.00	0.07 ± 0.02	0.04 ± 0.01	0.01 ± 0.01	98.50 ± 77.29	0.51 ± 0.27	0.12 ± 0.16	16.39	11.30	6.07	16.39	0.00	3.58	3.02	6.60	1.12
	may-19	12.31 ± 0.38	6.78 ± 0.20	28.08 ± 1.76	0.02 ± 0.00	0.01 ± 0.01	0.03 ± 0.02	0.02 ± 0.01	1.25 ± 0.96	0.64 ± 0.33	0.15 ± 0.17	15.23	10.70	5.64	15.23	3.47	1.80	1.09	2.89	1.42
	jun-19	8.46 ± 0.13	7.36 ± 0.03	25.92 ± 1.76	0.04 ± 0.01	0.01 ± 0.00	0.06 ± 0.01	0.00 ± 0.00	44.00 ± 51.12	0.85 ± 0.59	0.20 ± 0.21	15.09	14.00	5.59	15.09	1.60	2.40	1.37	3.77	2.06
	jul-19	8.80 ± 0.10	7.17 ± 0.03	25.38 ± 1.08	0.02 ± 0.01	0.01 ± 0.00	0.05 ± 0.00	0.00 ± 0.00	0.25 ± 0.50	0.84 ± 0.34	0.10 ± 0.13	17.09	12.00	6.33	17.09	0.67	1.81	1.20	3.01	1.18
	aug-19	8.41 ± 0.12	8.00 ± 0.05	24.84 ± 1.25	0.02 ± 0.02	0.01 ± 0.00	0.06 ± 0.03	0.00 ± 0.00	26.25 ± 16.88	1.00 ± 0.52	0.12 ± 0.18	16.50	12.40	6.11	16.50	0.00	2.30	1.45	3.75	1.70
	sep-19	10.61 ± 0.10	7.35 ± 0.21	26.08 ± 1.04	0.35 ± 0.26	0.01 ± 0.00	0.03 ± 0.01	0.00 ± 0.00	30.00 ± 11.97	0.84 ± 0.18	0.06 ± 0.10	18.04	10.80	6.68	18.04	0.80	0.51	0.21	0.72	0.64
	oct-19	10.84 ± 0.19	7.06 ± 0.01	32.20 ± 5.61	0.03 ± 0.03	0.01 ± 0.00	0.05 ± 0.01	0.00 ± 0.00	2.25 ± 3.30	0.75 ± 0.30	0.26 ± 0.29	15.39	11.60	5.70	15.39	0.27	1.64	1.58	3.22	0.12
	dec-19	12.51 ± 0.06	6.56 ± 0.21	27.12 ± 1.71	0.01 ± 0.00	0.01 ± 0.00	0.04 ± 0.01	0.00 ± 0.00	18.25 ± 6.13	0.87 ± 0.25	0.23 ± 0.29	12.96	10.20	4.80	12.96	1.54	2.23	2.23	4.46	0.00

3.1. Principal Component Analysis (PCA)

Regarding the Average Eigenvalue Criterion (AEC), two components (PCs) were identified, i.e., the optimal number of PCs. The percentage of explained variance for these two components were 70.1% and 13.8% for PC1 and PC2, respectively. Figure 2 shows the score plot of the PCA of each monthly record of both studied reservoirs. A clear distinction between both reservoirs is observed.

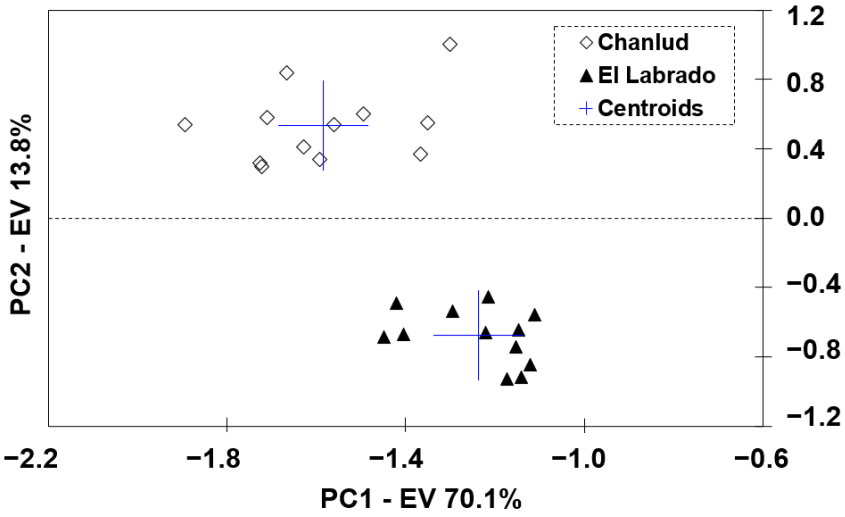


Figure 2. Score plot from the principal component analysis performed for the Chanlud and El Labrado reservoirs.

In Figure 2, the centroids of the coordinates of each reservoir are shown, (−1.59, 0.53) and (−1.24, −0.68) for Chanlud and El Labrado, respectively. The points for El Labrado are closer to their centroid than the points of the Chanlud reservoir, which are more dispersed from its centroid. This finding implies that fewer temporal (monthly) differences exist for El Labrado than for Chanlud. The average Euclidean distance between points belonging to the Chanlud reservoir and their centroid is 0.23 ± 0.13; meanwhile, for the points of El Labrado, it is 0.18 ± 0.07.

Eight informative variables were identified by the PCA (|loadings| > 0.25) that explain the variability of studied reservoirs (Table 2, Figure 3).

Table 2. Loading values for the principal components of the PCA model. Bold and italic values indicate a strong influence of the variables (i.e., |loadings| > 0.25). WT = water temperature, PPt = precipitation, D_{max} = maximum depth, Z_{sd} = Secchi disk, $CaCO_3$ = alkalinity, O_2 = dissolved oxygen, WF = wind force, PP = primary productivity, HB = heterotrophic bacteria, Chl = chlorophyll-*a*, and NO_3^--N = nitrate.

Parameter	PC1	PC2
WT	***−0.40***	−0.17
PPt	***−0.39***	0.06
D_{max}	***−0.38***	***0.54***
Z_{sd}	***−0.37***	***−0.40***
$CaCO_3$	***−0.36***	***0.40***
O_2	***−0.34***	−0.23
WF	***−0.27***	***−0.46***
PP	−0.23	***0.28***
HB	−0.13	−0.06
Chl	−0.12	−0.06
NO_3^--N	−0.06	0.07

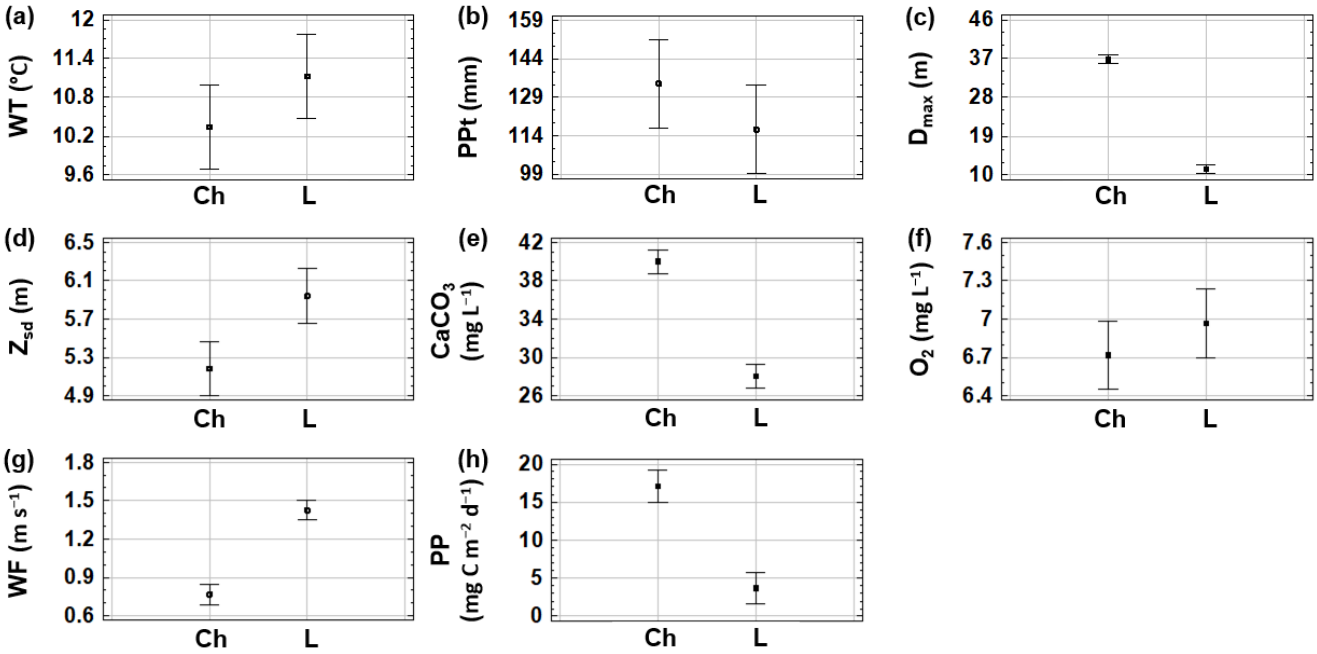


Figure 3. Means and Fisher's test-based intervals of the significant variables for studied reservoirs (Ch = Chanlud and L = El Labrado). (**a**) WT = water temperature, (**b**) PPt = precipitation, (**c**) D_{max} = maximum depth, (**d**) Z_{sd} = Secchi disk, (**e**) $CaCO_3$ = alkalinity, (**f**) O_2 = dissolved oxygen, (**g**) WF = wind force, and (**h**) PP = primary productivity. Mean values are depicted with a black point symbol.

Table 2 shows the informative variables for PC1 and PC2 based on the values of their loadings. Considering the percentage of explained variance for these two components (i.e., 70.1 and 13.8% for PC1 and PC2, respectively), the variables of PC1 have the most informative load to comparatively evaluate the studied reservoirs.

The mean values of the following parameters, WT (Figure 3a), Z_{sd} (Figure 3d), O_2 (Figure 3f), and WF (Figure 3g), were reported to be higher in El Labrado than Chanlud ($\bar{x}$ of WT expressed in °C is 11.1 for El Labrado and 10.3 °C for Chanlud; $\bar{x}$ of Z_{sd} is 5.9 m for El Labrado and 5.2 m for Chanlud; $\bar{x}$ of O_2 is 7.0 mg L^{-1} for El Labrado and 6.7 mg L^{-1} for Chanlud; and $\bar{x}$ of WF expressed in m s^{-1} is 1.4 for El Labrado and 0.8 for Chanlud). For precipitation (Figure 3b), D_{max} (Figure 3c), $CaCO_3$ (Figure 3e), and PP (Figure 3h), the inverse trend was observed ($\bar{x}$ of precipitation expressed in mm is 116.5 for El Labrado and 134.4 for Chanlud; $\bar{x}$ of D_{max} is 11.4 m for El Labrado and 36.7 m for Chanlud; $\bar{x}$ of $CaCO_3$ expressed in mg L^{-1} is 28.1 for El Labrado and 40.0 for Chanlud; and $\bar{x}$ of PP expressed in mg C m^{-2} d^{-1} is 3.7 for El Labrado and 17.1 for Chanlud). However, for the specific cases of WT (Figure 3a), precipitation (Figure 3b), and O_2 (Figure 3f), the intervals displayed around the mean based on Fisher's least significant difference (LSD) procedure overlap 95.0% of the time, indicating that nonsignificant differences exist between the means of those parameters. It is important to emphasize this finding because although WT, precipitation, and O_2 do not exhibit significant statistical differences between assessed reservoirs (Figures 3a, 3b, and 3f, respectively), they are parameters that, under the PCA, are key to explaining each reservoir's temporal variability.

Analysis of the Variables Identified by PCA as Informative to the Studied Reservoirs

With regard to meteorological parameters, for the Chanlud reservoir, the annual wind force (WF, Figure 4) ranged from 0.51 to 1.0 m s^{-1} ($\bar{x}$ = 0.8 ± 0.1 m s^{-1}). In many months, the WF was similar (range = 0.7–1, $\bar{x}$ = 0.9 ± 0.1 m s^{-1}). However, in the months of February, March, April, and May, the WF ranged from 0.5 to 0.7 m s^{-1}, with the mean value of 0.6 ± 0.1 m s^{-1} reported in those months. For El Labrado reservoir, the annual wind force (WF) ranged from 1.2 to 1.9 m s^{-1} ($\bar{x}$ = 1.4 ± 0.2 m s^{-1}) and was similar for most months (range = 1.2–1.4, $\bar{x}$ = 0.9 ± 0.1 m s^{-1}). However, a comparatively high WF was reported in June, July, and August and ranged from 1.6 to 1.9 m s^{-1} with a mean value of 1.7 ± 0.1 m s^{-1}. Regarding precipitation, in Chanlud, it ranges from 66.0 to 184.4 mm ($\bar{x}$ = 134.4 ± 35.8 mm), and for El Labrado, it ranges from 46.0 to 191.3 mm ($\bar{x}$ = 116.5 ± 44.9 mm). A seasonal trend was observed for El Labrado where for July, August, and September, the lowest precipitation was registered, $\bar{x}$ = 71 ± 22.8 mm (Figure 4).

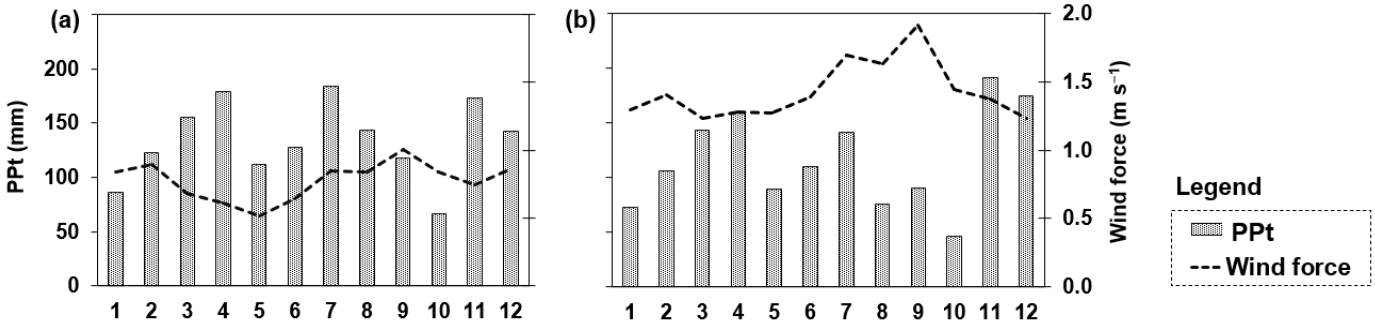


Figure 4. Monthly data of the cumulative precipitation (PPt) and the average wind force recorded in meteorological stations located in the proximity of the studied reservoirs: (**a**) Chanlud and (**b**) El Labrado in (1) December 2018 and (2) January, (3) February, (4) March, (5) April, (6) May, (7) June, (8) July, (9) August, (10) September, (11) October, and (12) December of 2019.

Vertical changes in the water temperature (WT) in the reservoir Chanlud are given in Figure 5. No evidence of consistent thermal stratification was observed. The coldest months were from June to October, and the mean temperature reported for this period was 9.0 ± 0.7 °C (Figure 5). The rest of the months reported a mean temperature of 11.6 ± 0.3 °C, i.e., the warmest period. The change in the temperature between the warmest period and the rest of the time is 2.6 °C. The maximum and minimum differences between the surface and the bottom were 2.9 and 0.9 °C in October and April, respectively. This emphasizes that mixing events are related to the warmest periods, and weak stratification occurs during colder times. Like WT, vertical profiles of dissolved oxygen (O_2) exhibit the highest values at the surface and the lowest O_2 concentrations at the bottom (Figure 5). A seasonal O_2 concentration is present, i.e., during the coldest period, a higher solubility of O_2 is notorious ($\bar{x}$ = 7.4 ± 0.4 mg L^{-1}), while, on the other hand, a lower O_2 solubility ($\bar{x}$ = 6.2 ± 0.3 mg L^{-1}) is associated with the warmest months. Water transparency by the Secchi disk (Z_{sd}) ranged between 4.2 and 6.6 m ($\bar{x}$ = 5.2 ± 0.8 m). The depth of the Chanlud reservoir ranged from 30.7 to 39.5 m, and the mean depth was reported as 36.8 ± 2.8 m. The euphotic zone (Z_{eu}) ranged from 13.0 to 18.0 m ($\bar{x}$ = 16.1 ± 2.0 m). The light vertical extinction coefficient (E_v) ranged from 0.2 to 0.3 ($\bar{x}$ = 0.24 ± 0.04) (these last two parameters were not significant regarding the PCA, namely, |loadings| < 0.25).

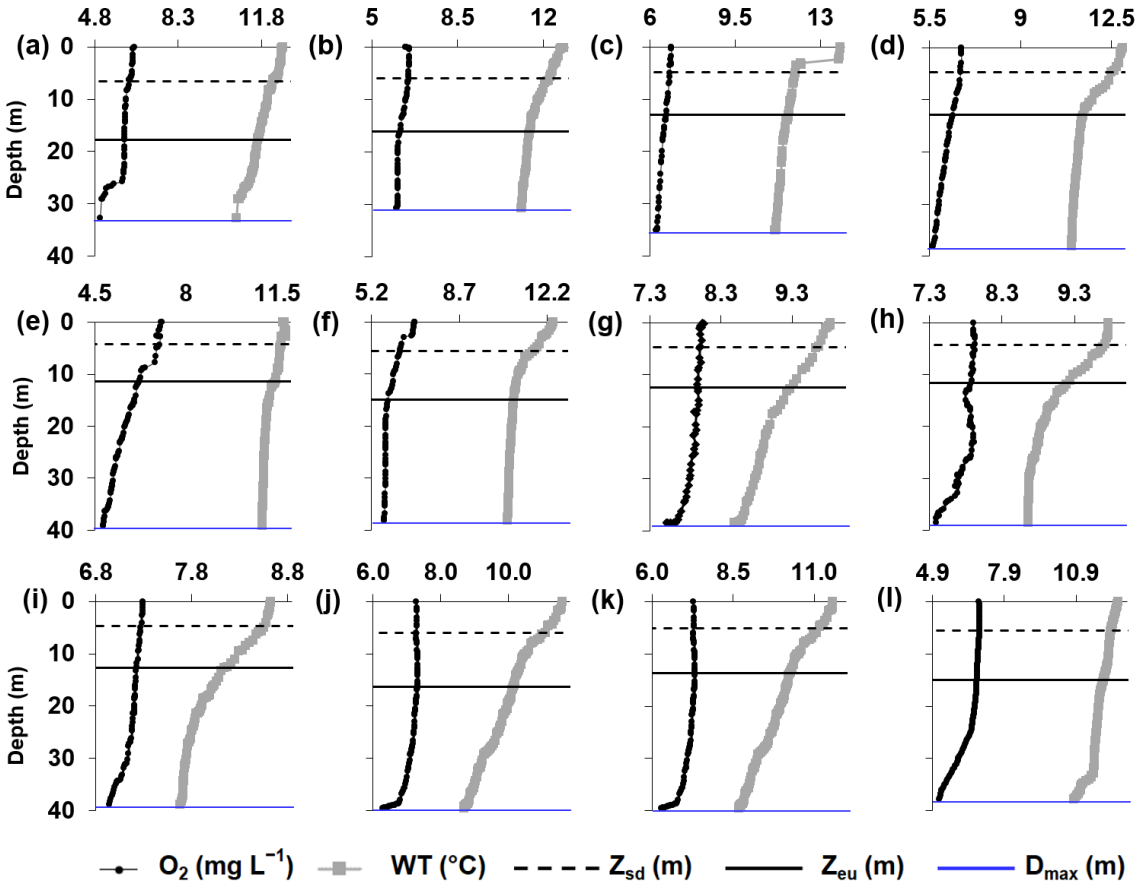


Figure 5. Monthly vertical profiles of dissolved oxygen (O_2) and water temperature (WT) of the Chanlud reservoir: depth of the Secchi disk (Z_{sd}), euphotic zone (Z_{eu}), and maximum depth (D_{max}) in (**a**) December 2018 and (**b**) January, (**c**) February, (**d**) March, (**e**) April, (**f**) May, (**g**) June, (**h**) July, (**i**) August, (**j**) September, (**k**) October, and (**l**) December of 2019.

The water temperature (WT) vertical profiles of El Labrado reservoir (Figure 6) show a typical curve, with the warmest water temperatures at the surface and the coldest at the bottom for most months. No thermic stratification is observed (with the exception of August, see Figure 6i). Evenly, in El Labrado reservoir, a clear thermic temporal trend is reflected, where, as in the case of Chanlud, June, July, August, September, and October are the coldest months ($\bar{x}$ = 9.4 ± 1.2 °C), and the rest of the months correspond with the warmest period ($\bar{x}$ = 12.4 ± 0.4 °C). There is a 3.0 °C difference between the warmest and coldest periods. The maximum and minimum differences between the surface and the bottom were 1.8 and 0.2 °C in March and December 2019, respectively. The vertical profiles of O_2 do not exhibit a trend regarding the depth gradient. Still, a seasonal O_2 concentration is present, where a higher solubility of O_2 is during the coldest period ($\bar{x}$ = 7.4 ± 0.4 mg L^{-1}). To the contrary, a lower O_2 solubility ($\bar{x}$ = 6.6 ± 0.1 mg L^{-1}) is associated with the warmest months. Z_{sd} ranged between 4.8 and 6.7 m ($\bar{x}$ = 6.0 ± 0.6 m), and the depth range values were between 8.4 and 14.1 ($\bar{x}$ = 11.4 ± 1.6 m). Z_{eu} was always greater than the maximum depth for El Labrado reservoir, and the E_v ranged from 0.2 to 0.3 ($\bar{x}$ = 0.2 ± 0.0.2).

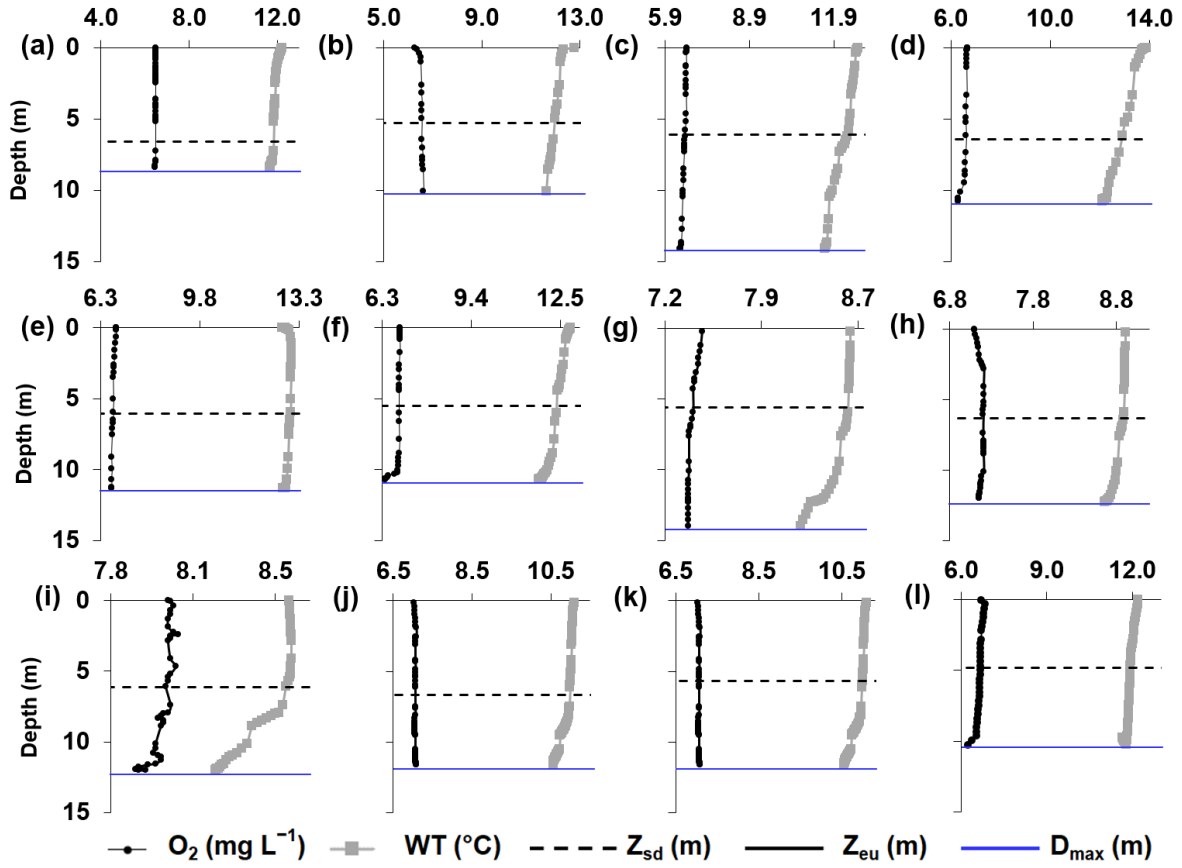


Figure 6. Monthly vertical profiles of dissolved oxygen (O_2) and water temperature (WT) of El Labrado reservoir: depth of the Secchi disk (Z_{sd}) and maximum depth (D_{max}) in (**a**) December 2018 and (**b**) January, (**c**) February, (**d**) March, (**e**) April, (**f**) May, (**g**) June, (**h**) July, (**i**) August, (**j**) September, (**k**) October, and (**l**) December of 2019.

The total alkalinity in Chanlud fluctuated between 32.4 and 85.0 mg L^{-1} of $CaCO_3$ ($\bar{x}$ = 40.6 ± 6.4 mg L^{-1}). No evidence of a trend regarding depth gradient exists for total alkalinity, and their maximum value was detected in January (i.e., 85.0 mg L^{-1} of $CaCO_3$). For El Labrado reservoir, the total alkalinity fluctuated between 23.8 and 38.8 mg L^{-1} of $CaCO_3$, with an overall mean of 27.9 ± 2.9 mg L^{-1}. No trend regarding depth gradient exists, and their maximum value was detected in October (i.e., 38.8 mg L^{-1} of $CaCO_3$).

Concerning primary productivity (PP), it was used as a single value in the PCA; however, in the current section, we approach this parameter according to its components (i.e., GPP + NPP = PP) to give the reader a more detailed description. Thus, the $\bar{x}$ gross primary productivity (GPP) value in the Chanlud reservoir was 9.9 ± 4.1 mg C m^{-2} d^{-1}, and for net primary productivity (NPP), the $\bar{x}$ = 7.2 ± 2.9 mg C m^{-2} d^{-1}. Higher values were found near the surface and decreased irregularly to the bottom. For the temporal component, a downward trend in GPP and NPP was observed during the coldest period (i.e., for the warm period, $\bar{x}_{GPP}$ = 11.8 ± 4.3 mg C m^{-2} d^{-1}; $\bar{x}_{NPP}$ = 8.5 ± 3.1 mg C m^{-2} d^{-1}; for the cold period, $\bar{x}_{GPP}$ = 7.3 ± 2.0 mg C m^{-2} d^{-1}; $\bar{x}_{NPP}$ = 5.3 ± 1.4 mg C m^{-2} d^{-1}) (see Figure 7a).

For El Labrado reservoir, the $\bar{x}_{GPP}$ = 2.1 ± 0.8 mg C m^{-2} d^{-1}, and for NPP, it was 1.5 ± 0.7 mg C m^{-2} d^{-1}. As in the case of the Chanlud reservoir, seasonality is essential to explain the trends in GPP and NPP—namely, for the warm period, $\bar{x}_{GPP}$ = 2.4 ± 0.8 mg C m^{-2} d^{-1}; $\bar{x}_{NPP}$ = 1.8 ± 0.7 mg C m^{-2} d^{-1}; for the cold period, $\bar{x}_{GPP}$ = 1.7 ± 0.8 mg C m^{-2} d^{-1}; $\bar{x}_{NPP}$ = 1.2 ± 0.5 mg C m^{-2} d^{-1} (Figure 7b).

Concerning the respiration (R) rates for the Chanlud reservoir, X_R = 7.4 ± 6.2 mg C m^{-2} d^{-1}. For the warm period, $\bar{x}_R$ = 9.4 ± 7.1 mg C m^{-2} d^{-1}, and for the cold period, $\bar{x}_R$ = 4.7 ±

3.8 mg C m^{-2} d^{-1}. The mean R rate in El Labrado reservoir was 1.2 0.9 ± 0.9 mg C m^{-2} d^{-1}. However, contrary to the Chanlud reservoir pattern, seasonality marginally influences R in this reservoir (i.e., for the warm period, $\bar{x}_R$ = 1.3 ± 1.0 mg C m^{-2} d^{-1} and for the cold period, $\bar{x}_R$ = 1.1 ± 0.8 mg C m^{-2} d^{-1}) (R was not significant regarding the PCA, i.e., |loadings| < 0.25).

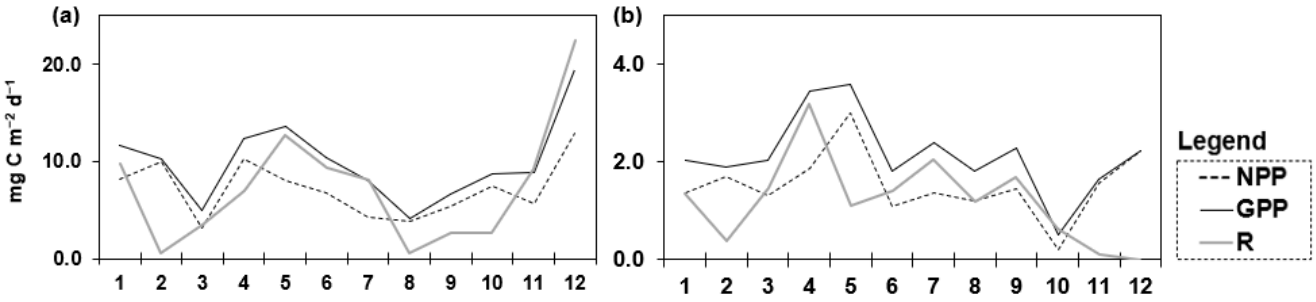


Figure 7. Gross primary productivity (GPP), net primary productivity (NPP), and respiration (R) rates for each month at the (**a**) Chanlud and (**b**) El Labrado reservoirs in (1) December 2018 and (2) January, (3) February, (4) March, (5) April, (6) May, (7) June, (8) July, (9) August, (10) September, (11) October, and (12) December of 2019.

3.2. Multiple Linear Regression Analysis (MLRA)

Concerning the individual MLRAs performed for each reservoir, the Adjusted R-Squared (Adj—R^2) values were 0.7 and 0.8 for the Chanlud ($MLRA_{Ch}$) and El Labrado ($MLRA_L$) regression models, respectively, which implies that the models, as fitted, very well explain the variability in PP in both cases. The Durbin–Watson (DW) statistic value was 2.1 in both cases, which is congruent with the absence of serial autocorrelation in the residuals at the 95.0% confidence level (the DW statistic becomes smaller as the serial correlation increases). The *p*-values of the analysis of variance of both cases were less than 0.05 (i.e., 0.04 for $MLRA_{Ch}$ and $MLRA_L$); therefore, there are statistically significant relationships between the independent variables and PP at the 95.0% confidence level in both models.

The output equation of the fitted model for the Chanlud reservoir is as follows:

$$PP_{Ch} = -5.39 + 0.87 \times WT + 3.87 \times D_{max} + 1.14 \times Chl + 1.66 \times Alkalinity + 0.75 \times HB + 1.70 \times WF$$

and for El Labrado reservoir, it is as follows:

$$PP_L = -0.26 - 0.31 \times O_2 + 0.12 \times WT + 0.12 \times HB + 0.09 \times Precipitation + 0.60 \times WF$$

Different planned approaches were designed for PCA and MLRAs in the current research; despite this, both analyses choose similar variables as informative to perform their corresponding modeling. For example, WT, precipitation, and O_2 are critical variables according to the PCA to describe the seasonal variability of both reservoirs and are equally chosen by MLRAs as crucial variables to explain the variability of the PP in the studied reservoirs. Also, D_{max}, $CaCO_3$, and WF are all critical variables identified by the PCA to perform a clear discrimination between both reservoirs. MLRAs equally choose them as the most informative variables to explain the variability of the PP in the evaluated reservoirs.

Nevertheless, notwithstanding these similarities, each reservoir itself has its own set of descriptive parameters to explain the variability of its corresponding PP trends. Hence, checking the output MLRA equations shows that Chanlud is more complex than El Labrado, not only due to the number of variables but also due to their nature. For example, the hydraulic and chemical components in Chanlud are more critical than in El Labrado; conversely, the metrological component in El Labrado is more relevant than in Chanlud. Orographic factors (the almost complete absence of hills around Chanlud, which is opposite El Labrado) and the critical size difference between the contributing hydrological areas

of both reservoirs (for Chanlud, the contributing hydrological area is 85.5 km^2, and for El Labrado, it is 42.0 km^2) could explain these differences in terms of complexity between both multiple regression analyses ($MLRA_{Ch}$ and $MLRA_L$).

On the other hand, in both MLRAs, some variables identified as not significant by the PCA (i.e., |loadings| < 0.25) were chosen as essential to explain the variability of the PP (i.e., heterotrophic bacteria and chlorophyll-α, HB and Chl, respectively). Thus, for Chanlud, values of HB were found between 0 and 250 with a mean value of 21.6 ± 39.2 bacteria 100^{-1} mL^{-1}. The highest values were found in July and September (250 and 141 bacteria 100^{-1} mL^{-1}, respectively). In the case of El Labrado reservoir, the heterotrophic bacteria were found in a range of 0 to 190 bacteria 100^{-1} mL^{-1} with a mean value of 19.5 ± 36.8 bacteria 100^{-1} mL^{-1} (Table 1). The highest values were found in April and June (190 and 120 bacteria 100^{-1} mL^{-1}, respectively). Both reservoirs showed non-trends in HB concerning depth gradients. The chlorophyll-*a* (Chl) measurements in the Chanlud reservoir ranged from 0.4 to 6.2, with a mean of 1.7 ± 1.6 μg L^{-1}, while it ranged from 0 to 3.5, with a mean of 1.1 ± 1.1 μg L^{-1} in El Labrado reservoir (Table 1).

4. Discussion

In Ecuador, there are no previous studies that address the issue of limnology in reservoirs, and the availability of baseline data are restricted only to lakes [27,72–76]. This present paper is a pioneer effort to address the study of limnological aspects in high Andean reservoirs in Ecuador and one of the few references to tropical Andean reservoirs [16,21].

Both statistical approaches used in this research, i.e., the principal components analysis (PCA) and multiple linear regression analysis (MLRA), gave relevant results in selecting appropriate explanatory variables representative to (i) explain the seasonal variability of each reservoir, the (ii) potential differences between the two studied reservoirs, and (iii) the variability of the PP in each reservoir. Furthermore, the high values of their performance statistics validate the scientific reliability of the outputs.

For both reservoirs, the monthly mean values of dissolved oxygen and water temperature followed temporal patterns previously reported for reservoirs and lakes; namely, the higher the temperature, the lower the diffusion of dissolved oxygen and vice versa [77,78]. Additionally, both variables exhibited a downward trend regarding depth; however, no thermal stratification was observed, which implies frequent mixing events, probably due to strong winds (wind force was a variable that both PCA and MLRAs chose as informative) and the lack of hills or mountains around the reservoirs [21], mainly in Chanlud. The downward pattern of dissolved oxygen regarding depth was weaker in El Labrado than in Chanlud; however, no statistically significant differences existed for this parameter between both reservoirs (Figure 3f). This last finding can be partially explained, considering that wind force is significantly higher in El Labrado than in the Chanlud reservoir (Figure 3g). Similar to most tropical lakes, the thermal stratification of the water column in both reservoirs is typically weak due to limited seasonal variation in temperature [79]. Thus, in tropical Andean reservoirs, the high and cold inflows during the wet season homogenize the water column below a shallow surface mixed layer; in dry seasons, warmer inflows enter at intermediate depths, favoring the development of a thick metalimnion with sharper temperature gradients at its top and base [20,77,80,81]. Our results did not show this seasonal trend. Other studies in the lakes of Cajas National Park, near the area of this current research, identified the same colder period; however, contrary to this study, the authors linked this period with the thermal stratifications of some of the studied lakes [76]. The differences in the flushing time of water bodies and the effects of riverine inflows at the studied sites could explain this non-congruence between both studies.

Concerning nutrients, only nitrates were representative of signal chemical detection. Nitrates were most notorious in the Chanlud reservoir (i.e., the mean of nitrates for Chanlud is 0.56 ± 1.52 mg L^{-1}, and for El Labrado, it is 0.06 ± 0.12 mg L^{-1}). We interpret the increased availability of nitrates in Chanlud as mainly the result of the notoriously larger size of their contributing hydrological area relative to El Labrado. Thus, higher rates of

organic material production in the terrestrial part of the catchment subsequently increase the leaching of nitrates into aquatic systems [82,83]. However, despite the nitrate concentrations detected, their values were generally consistent with very low concentrations, which is congruent with the fact that both PCA and MLRAs considered nitrates a nonsignificant variable. The rest of the nutrients (i.e., nitrites, ammonium, and orthophosphates) presented weak chemical signals (Table 1). Two explanations are provided in this regard: (i) In tropical regions, in the first rainy season, many nutrients are carried into reservoirs by the first precipitations. A peak in nutrient input can often be attributed to surface runoff from nutrient-rich soils [84]. However, most of these nutrients will not remain in the system for long if the residence time of the water is short, i.e., if there is a high flushing rate, as is the case in many reservoirs. (ii) There is an almost complete absence of human populations in the region's reservoirs [85]; i.e., the contributing hydrological areas for both reservoirs are highly conserved. Their landscapes are conformed by pristine ecosystems (for Chanlud, 0.3% of their contributing basin is anthropized, and for El Labrado, the percentage is 0.5%) [86].

Regarding alkalinity, the current outputs are congruent with other Andean lentic systems, such as La Brava and La Punta lakes in northern Chile, where very similar values were reported [87]. Thus, the current results suggest that for both reservoirs, the waters are slightly alkaline, especially Chanlud (Figure 3e). In this context, the more alkaline a lake is, the greater the concentration of carbonates [88], which has been reported as a promoter of the growth of many groups of phytoplankton [89,90]. This is consistent with this study's findings, where a congruence between trends in alkalinity and primary productivity (Figure 3e,h) was observed for both reservoirs. Furthermore, concerning the $MLRA_{Ch}$, alkalinity is an important explanatory variable to explain the variability of primary productivity.

For water transparency (Z_{sd}), there was a difference between the monthly measurements of both reservoirs. El Labrado reservoir contained the most transparent waters (Figure 3d), which could be explained by the lowest nutrient concentration and primary productivity (Figure 3h) in this reservoir compared to Chanlud. Furthermore, this finding could be explained by the contributing hydrological areas of both reservoirs (86.8 and 40.1 km^2 for Chanlud and El Labrado, respectively); i.e., the greater the contribution area, the greater the runoff area, and therefore, the greater the amounts of total solids going into the reservoir. Despite this, the reservoirs' current water transparency values were slightly lower than reported in the lakes of the Cajas National Park, Z_{sd} $\bar{x}$ = 6.7 m [76].

Regarding the primary productivity (PP) values, $PP_{Chanlud} > PP_{El\ Labrado}$ (Figure 3h). The outputs for PP correspond with low ecosystem metabolic activity and a low loading nutrient rate. In general, in lakes and reservoirs, it has been reported that low PP occurs when (i) human activities in the surrounding areas are scarce, (ii) as a product of wind stress, (iii) when there is no stability concerning solar radiation, and (iv) as a product of non-effective nutrient recycling [91–93]. This latter factor is congruent with findings for twenty-four tropical high-altitude lakes in southern Ecuador [94]. In this study, the authors found that lower phosphate concentrations explain the low productivity of the studied lakes, which is consistent with our findings in the studied reservoirs, where the phosphates (among other nutrients) were undetectable. In addition to these four factors, two more explanatory elements must be included for this current study case: (v) the relatively short water residence times and (vi) the fact that both reservoirs are above 3400 m a.s.l. Hence, despite the low PP values obtained, the PP method efficiently captured increased and decreased dissolved oxygen data in the clear and dark bottles. It is necessary to consider that current PP datasets are expected to be typical of the Andean lentic water bodies, mainly due to their pristine conditions and altitudinal factors The latter is congruent with findings for northern Sweden lakes, where the PP decreases as altitude increases [95]. Unfortunately, very few studies on similar reservoirs in physiographic terms to those studied in this research have been conducted in order to be able to perform a comparative analysis (mainly in the Andean region). However, some findings about metabolic rates in

this current research are congruent with other studies. For example, in the case of Lake Monte Alegre (south-eastern Brazil), a study reported that the higher PP in the water column occurred in the transition periods when thermal stratification was unstable and lower PP occurred in the cold season (frequent mixing) [96]. Both findings are congruent with the outputs of the two studied reservoirs. In Chanlud, the peak of PP is just after the coldest period, and for El Labrado, it is before it (Figure 7); i.e., timing/season is essential. Thus, for Chanlud, during the coldest months, the $\bar{x}_{PP}$ = 12.6 mg C m^{-2} d^{-1}, and in the warmest period, the $\bar{x}_{PP}$ = 20.3 mg C m^{-2} d^{-1}; for El Labrado, for the coldest months, $\bar{x}_{PP}$ = 2.9 mg C m^{-2} d^{-1}, and for the warmest period, $\bar{x}_{PP}$ = 4.2 mg C m^{-2} d^{-1}. These results are consistent with more studies carried out in other lakes and reservoirs, where the same PP and water temperature relationship was observed [97,98] (herein, the MLRAs chose water temperature as one of the critical parameters to explain the variability of PP in both reservoirs). In this context, the PP in the studied reservoirs is subject to multifactorial regulation. Besides water temperature, meteorological (i.e., wind force, precipitation) and biological (i.e., heterotrophic bacteria) factors describe the PP and their variability. This is like other studies, where there is evidence that a set of variables (like the ones reported here) have been described as determining factors in regulating biological processes in the lakes of the Andes [73,99,100].

Following a statistically sound approach, this study aims to increase our understanding of the limnological characteristics of tropical high Andean reservoirs, which have yet to be studied in much detail. The results will also form an important baseline for information to determine future changes that might take place in them, such as climatic changes, which are predicted to be dramatic at high latitudes [101], and local stressors. Also, this research identifies significant and nonsignificant descriptive variables to describe (i) the variability of each reservoir and discriminatory factors between them and (ii) the primary productivity of the studied reservoirs. Both findings have the potential to reduce the number of variables to be monitored in future similar research and, consequently, the monitoring time and related monetary expenses.

5. Conclusions

Some differences are evident between both reservoirs in aspects related to physicochemical (i.e., alkalinity, light penetration) and biological factors (i.e., primary productivity). Chanlud exhibits a more photosynthetically efficient euphotic zone. Although the primary productivity of Chanlud was higher than El Labrado, the results for both reservoirs correspond to low metabolic rates. This was expected since primary productivity rates are linked to the intrinsic conditions of reservoirs, that is, high elevation, low nutrient recycling, low temperatures, wind stress, and short retention times. The method used to estimate the metabolic rates of the reservoirs was practical and provided representative and reliable information. This is validated by contrasting the vertical integrations of primary productivity with variables such as temperature and dissolved oxygen. Temperature, heterotrophic bacteria, and wind force are critical variables in both reservoirs since the results significantly influence primary productivity rates. The study's weaknesses include its reliance on accessible areas near dam walls. Incorporating new sampling sites associated with a horizontal zonation of reservoirs would benefit future evaluations. Also, more accurate methodologies to measure the primary productivity and respiration rates could be tested—for example, the oxygen isotope ($\delta^{18}O$) mass balance approach.

Author Contributions: Conceptualization, G.S.; Methodology, G.S., J.R., C.L., M.A.E.F. and P.L.M.G.; Software, G.S.; Formal analysis, G.S.; Investigation, G.S. and J.R.; Data curation, G.S. and J.R.; Writing—original draft, G.S.; Writing—review & editing, G.S., A.A., C.L., M.A.E.F. and P.L.M.G.; Supervision, A.A., C.L., M.A., M.A.E.F. and P.L.M.G.; Project administration, A.A. and M.A.; Funding acquisition, A.A. and M.A. All authors have read and agreed to the published version of the manuscript.

Funding: The APC was kindly paid by the Universidad Hemisferios. Not specific grant number applicable.

Data Availability Statement: The data might be available directly from the Departamento de Recursos Hídricos y Ciencias Ambientales of the Universidad de Cuenca.

Acknowledgments: The authors would like to thank the company Electro Generadora del Austro (Elecaustro S.A.) and the University of Cuenca for funding this current study. The preparation of the manuscript took place under the framework of the project "Investigación biótica, metabólica y trófica de los embalses de Chanlud y El Labrado".

Conflicts of Interest: Author Marta Aguilar was employed by the company Empresa Electro Generadora del Austro (Elecaustro S. A.). The remaining authors declare that the research was conducted in the absence of any commercial or financial relationships that could be construed as a potential conflict of interest.

References

1. Rodgher, S.; Espíndola, E.L.; Rocha, O.; Fracácio, R.; Pereira, R.H.; Rodrigues, M.H. Limnological and ecotoxicological studies in the cascade of reservoirs in the Tietê River (São Paulo, Brazil). *Braz. J. Biol.* **2005**, *65*, 697–710. [CrossRef] [PubMed]
2. Zarfl, C.; Lumsdon, A.E.; Berlekamp, J.; Tydecks, L.; Tockner, K. A global boom in hydropower dam construction. *Aquat. Sci.* **2015**, *77*, 161–170. [CrossRef]
3. Bredenhand, E.; Samways, M.J. Impact of a dam on benthic macroinvertebrates in a small river in a biodiversity hotspot: Cape Floristic Region, South Africa. *J. Insect Conserv.* **2009**, *13*, 297–307. [CrossRef]
4. Nguyen, T.H.T.; Everaert, G.; Boets, P.; Forio, M.A.E.; Bennetsen, E.; Volk, M.; Hoang, T.H.T.; Goethals, P.L.M. Modelling tools to analyze and assess the ecological impact of hydropower dams. *Water* **2018**, *10*, 259. [CrossRef]
5. Margalef, R. *Limnología*; Omega: Barcelona, Spain, 1983.
6. Bengtsson, L.; Herschy, R.W.; Fairbridge, R.W. *Encyclopedia of Lakes and Reservoirs*; Springer: Dordrecht, The Netherland, 2012.
7. Simões, N.R.; Nunes, A.H.; Dias, J.D.; Lansac-Tôha, F.A.; Velho, L.F.M.; Bonecker, C.C. Impact of reservoirs on zooplankton diversity and implications for the conservation of natural aquatic environments. *Hydrobiologia* **2015**, *758*, 3–17. [CrossRef]
8. Song, C.; Gardner, K.H.; Klein, S.J.W.; Souza, S.P.; Mo, W. Cradle-to-grave greenhouse gas emissions from dams in the United States of America. *Renew. Sustain. Energy Rev.* **2018**, *90*, 945–956. [CrossRef]
9. Dodds, W.K.; Whiles, M.R. *Freshwater Ecology*; Academic Press: Cambridge, MA, USA, 2019.
10. Páez, R.; Ruiz, G.; Márquez, R.; Soto, L.M.; Montiel, M.; López, C. Limnological studies on a shallow reservoir in Western Venezuela (Tulé Reservoir). *Limnologica* **2001**, *31*, 139–145. [CrossRef]
11. Silva, R.F.C.M.; de Almeida, T.; Cicerelli, R.E.; Gomes, L.N.L. A spatiotemporal analysis of the physicochemical parameters after the operation of the Corumbá IV reservoir (Midwest Brazil) to support better management decision. *Environ. Monit. Assess.* **2021**, *193*, 247. [CrossRef] [PubMed]
12. Williamson, C.E.; Saros, J.E.; Vincent, W.F.; Smol, J.P. Lakes and reservoirs as sentinels, integrators, and regulators of climate change. *Limnol. Oceanogr.* **2009**, *54*, 2273–2282. [CrossRef]
13. Soares, M.C.S.; Marinho, M.M.; Huszar, V.L.M.; Branco, C.W.C.; Azevedo, S.M.F.O. The effects of water retention time and watershed features on the limnology of two tropical reservoirs in Brazil. *Lakes Reserv. Res. Manag.* **2008**, *13*, 257–269. [CrossRef]
14. Gansser, A. Facts and theories on the andes. *J. Geol. Soc.* **1973**, *129*, 93–131. [CrossRef]
15. Michelutti, N.; Tapia, P.M.; Labaj, A.L.; Grooms, C.; Wang, X.; Smol, J.P. A limnological assessment of the diverse waterscape in the Cordillera Vilcanota, Peruvian Andes. *Inland Waters* **2019**, *9*, 395–407. [CrossRef]
16. Aguilera, X.; Declerck, S.; De Meester, L.; Maldonado, M.; Ollevier, F. Tropical high Andes lakes: A limnological survey and an assessment of exotic rainbow trout (Oncorhynchus mykiss). *Limnologica* **2006**, *36*, 258–268. [CrossRef]
17. Cabrol, N.A.; Grin, E.A.; Chong, G.; Minkley, E.; Hock, A.N.; Yu, Y.; Bebout, L.; Fleming, E.; Häder, D.P.; Demergasso, C.; et al. The High-Lakes Project. *J. Geophys. Res. Biogeosci.* **2009**, *114*, G00D06. [CrossRef]
18. Fortner, S.K.; Mark, B.G.; McKenzie, J.M.; Bury, J.; Trierweiler, A.; Baraer, M.; Burns, P.J.; Munk, L. Elevated stream trace and minor element concentrations in the foreland of receding tropical glaciers. *Appl. Geochem.* **2011**, *26*, 1792–1801. [CrossRef]
19. Benito, X.; Fritz, S.C.; Steinitz-Kannan, M.; Tapia, P.M.; Kelly, M.A.; Lowell, T.V. Geo-climatic factors drive diatom community distribution in tropical South American freshwaters. *J. Ecol.* **2018**, *106*, 1660–1672. [CrossRef]
20. Marín-Ramírez, A.; Gómez-Giraldo, A.; Román-Botero, R. Variación estacional de la temperatura media y los flujos advectivos y atmosféricos de calor en un embalse tropical andino. *Rev. Acad. Colomb. Cienc. Exactas Físicas Nat.* **2020**, *44*, 360–375. [CrossRef]
21. Villabona-González, S.L.; Benjumea-Hoyos, C.A.; Gutiérrez-Monsalve, J.A.; López-Muñoz, M.T.; González, E.J. Main physico-chemical and biological variables in the trophic state of five Colombian Andean reservoirs. *Rev. Acad. Colomb. Cienc. Exactas Físicas Nat.* **2020**, *44*, 344–359.
22. Tundisi, J.G.; Matsumura-Tundisi, T.; Calijuri, M.C. Limnology and management of reservoirs in Brazil. *Comp. Reserv. Limnol. Water Qual. Manag.* **1993**, *1000*, 25–55.
23. Tundisi, J.G.; Matsumura-Tundisi, T. Integration of research and management in optimizing multiple uses of reservoirs: The experience in South America and Brazilian case studies. *Hydrobiologia* **2003**, *500*, 231–242. [CrossRef]
24. Agostinho, A.A.; Gomes, L.C.; Latini, J.D. Fisheries management in brazilian reservoirs: Lessons from/for South America. *Interciencia* **2004**, *29*, 334–338.

25. Almeida, V.L.S.; Dantas, Ê.W.; Melo-Júnior, M.; Bittencourt-Oliveira, M.C.; Moura, A.N. Zooplanktonic community of six reservoirs in northeast Brazil. *Braz. J. Biol.* **2009**, *69*, 57–65. [CrossRef] [PubMed]
26. Tundisi, J.G. Reservoirs: New challenges for ecosystem studies and environmental management. *Water Secur.* **2018**, *4–5*, 1–7.
27. Steinitz-Kannan, M.; López, C.; Jacobsen, D.; Guerra, M.L. History of limnology in Ecuador: A foundation for a growing field in the country. *Hydrobiologia* **2020**, *847*, 4191–4206. [CrossRef]
28. Hwang, S.-J.; Kwun, S.-K.; Yoon, C.-G. Water quality and limnology of Korean reservoirs. *Paddy Water Environ.* **2003**, *1*, 43–52. [CrossRef]
29. Ulloa, C.; Jørgensen, P. *Arboles y Arbustos de los Andes del Ecuador*; Ediciones ABYA-YALA: Quito, Ecuador, 2002.
30. Buytaert, W.; Célleri, R.; De Bièvre, B.; Cisneros, F.; Wyseure, G.; Deckers, J.; Hofstede, R. Human impact on the hydrology of the Andean páramos. *Earth-Sci. Rev.* **2006**, *79*, 53–72. [CrossRef]
31. Buytaert, W.; Celleri, R.; Willems, P.; De Bièvre, B.; Wyseure, G. Spatial and temporal rainfall variability in mountainous areas: A case study from the south Ecuadorian Andes. *J. Hydrol.* **2006**, *329*, 413–421. [CrossRef]
32. Matute-Pinos, V.O. Análisis de Factibilidad de Generación Eléctrica a pie de la Presa de Chanlud. Bachelor's Thesis, Universidad de Cuenca, Cuenca, Ecuador, 2014.
33. Herrera, I.A.; Burneo, P. Environmental flow assessment in Andean rivers of Ecuador, case study: Chanlud and El Labrado dams in the Machángara River. *Ecohydrol. Hydrobiol.* **2017**, *17*, 103–112. [CrossRef]
34. American Public Health Association. *Standard Methods for the Examination of Water and Wastewater*, 20th ed.; American Public Health Association: Washington, DC, USA, 1998; Volume 34.
35. Massa, S.; Caruso, M.; Trovatelli, F.; Tosques, M. Comparison of plate count agar and R2A medium for enumeration of heterotrophic bacteria in natural mineral water. *World J. Microbiol. Biotechnol.* **1998**, *14*, 727–730. [CrossRef]
36. Snazelle, T. *Evaluation of Xylem EXO Water-Quality Sondes and Sensors*; USGS: Reston, VA, USA, 2015.
37. de Castro Medeiros, L.; Mattos, A.; Lürling, M.; Becker, V. Is the future blue-green or brown? The effects of extreme events on phytoplankton dynamics in a semi-arid man-made lake. *Aquat. Ecol.* **2015**, *49*, 293–307. [CrossRef]
38. Campos-Silva, J.V.; Peres, C.A.; Amaral, J.H.F.; Sarmento, H.; Forsberg, B.; Fonseca, C.R. Fisheries management influences phytoplankton biomass of Amazonian floodplain lakes. *J. Appl. Ecol.* **2021**, *58*, 731–743. [CrossRef]
39. Dokulil, M.; Silva, I.; Bauer, K. An assessment of the phytoplankton biomass and primary productivity of Parakrama Samudra, a shallow man-made lake in Sri Lanka. In *Limnology of Parakrama Samudra—Sri Lanka*; Springer: Dordrecht, The Netherland, 1983; pp. 49–76.
40. Amarasinghe, P.B.; Vijverberg, J. Primary production in a tropical reservoir in Sri Lanka. *Hydrobiologia* **2002**, *487*, 85–93. [CrossRef]
41. Wetzel, R.G.; Likens, G.E. *Limnological Analyses*, 3rd ed.; Springer Science+Business Media, LLC: New York, NY, USA, 1993.
42. Egna, H.S.; Boyd, C.E. *Dynamics of Pond Aquaculture*; CRC Press: Boca Raton, FL, USA, 1997.
43. Villarreal-Quintero, E.Y.; Alcocer, J.; Oseguera, L.A. Producción primaria en un lago oligotrófico tropical. In *Estado Actual del Conocimiento del Ciclo del Carbono y sus Interacciones en México: Síntesis a 2013*; Programa Mexicano del Carbono A.C.: Texcoco, Mexico, 2014; pp. 322–327.
44. Lehman, J.T. Hypolimnetic metabolism in Lake Washington: Relative effects of nutrient load and food web structure on lake productivity. *Limnol. Oceanogr.* **1988**, *33*, 1334–1347. [CrossRef]
45. Sterner, R.W. In situ-measured primary production in Lake Superior. *J. Great Lakes Res.* **2010**, *36*, 139–149. [CrossRef]
46. Lee, H.; Shum, C.K.; Tseng, K.H.; Guo, J.Y.; Kuo, C.Y. Present-day lake level variation from envisat altimetry over the northeastern qinghai-tibetan plateau: Links with precipitation and temperature. *Terr. Atmos. Ocean. Sci.* **2011**, *22*, 169–175. [CrossRef]
47. Larson, R.; Edwards, B.H.; Falvo, D.C. *Calculus I with Precalculus—A One-Year Course*, 3rd ed.; Brooks/Cole, Cengage Learning: Pacific Grove, CA, USA, 2011.
48. Hanselman, D.; Littlefield, B. *Mastering MATLAB®*; Pearson Education Limited: London, UK, 2012.
49. Wondie, A.; Mengistu, S.; Vijverberg, J.; Dejen, E. Seasonal variation in primary production of a large high altitude tropical lake (Lake Tana, Ethiopia): Effects of nutrient availability and water transparency. *Aquat. Ecol.* **2007**, *41*, 195–207. [CrossRef]
50. Shapiro, S.S.; Wilk, M.B. An Analysis of Variance Test for Normality (Complete Samples). *Biom. Trust.* **1965**, *52*, 591–611. [CrossRef]
51. Anderson, T.; Finn, J. *The New Statistical Analysis of Data*; Springer: New York, NY, USA, 1996.
52. Helsel, D.R.; Hirsch, R.M.; Ryberg, K.R.; Archfield, S.A.; Gilroy, E.J. Statistical Methods in Water Resources. In *Book 4, Hydrologic Analysis and Interpretation*; U.S. Geological Survey: Reston, VA, USA, 2020; p. 458.
53. R Core Team. *Package 'stats'*; R Core Team: Vienna, Austria, 2016.
54. Shen, C.; Shi, Y.; Fan, K.; He, J.-S.; Adams, J.M.; Ge, Y.; Chu, H. Soil pH dominates elevational diversity pattern for bacteria in high elevation alkaline soils on the Tibetan Plateau. *FEMS Microbiol. Ecol.* **2019**, *95*, fiz003. [CrossRef] [PubMed]
55. Frank, I.E.; Todeschini, R. *The Data Analysis Handbook*; Elsevier Science B.V.: Amsterdam, The Netherlands, 1994; Volume 14.
56. Zupan, J. *PCs for Chemists*; Elsevier Science Publishers B.V.: Amsterdam, The Netherlands, 1990; Volume 5.
57. Varmuza, K.; Filzmoser, P. *Introduction to Multivariate Statistical Analysis in Chemometrics*; Taylor & Francis Group, LLC.: Abingdon, UK, 2010; Volume 64.
58. Einax, J.W.; Zwanziger, H.W.; Geiss, S. *Chemometrics in Environmental Analysis*; Wiley-VCH Verlag GmbH: Hoboken, NJ, USA, 1997.

59. Ballabio, D. A MATLAB toolbox for Principal Component Analysis and unsupervised exploration of data structure. *Chemom. Intell. Lab. Syst.* **2015**, *149*, 1–9. [CrossRef]
60. Ballabio, D.; Consonni, V. Classification tools in chemistry. Part 1: Linear models. PLS-DA. *Anal. Methods* **2013**, *5*, 3790–3798. [CrossRef]
61. Mevik, B.; Wehrens, R. Introduction to the pls Package. In *Help Section of the "Pls" Package of R Studio Software*; R Core Team: Vienna, Austria, 2015; Section 7; pp. 1–23.
62. Rácz, A.; Bajusz, D.; Héberger, K. Modelling methods and cross-validation variants in QSAR: A multi-level analysis. *SAR QSAR Environ. Res.* **2018**, *29*, 661–674. [CrossRef] [PubMed]
63. Rani, M.; Marchesi, C.; Federici, S.; Rovelli, G.; Alessandri, I.; Vassalini, I.; Ducoli, S.; Borgese, L.; Zacco, A.; Bilo, F.; et al. Miniaturized near-infrared (MicroNIR) spectrometer in plastic waste sorting. *Materials* **2019**, *12*, 2740. [CrossRef] [PubMed]
64. Peres-Neto, P.R.; Jackson, D.A.; Somers, K.M. Giving meaningful interpretation to ordination axes: Assessing loading significance in principal component analysis. *Ecology* **2003**, *84*, 2347–2363. [CrossRef]
65. Chatfield, C.; Collins, A.J. *Introduction to Multivariate Analysis*, 1st ed.; Chapman and Hall: London, UK, 1980.
66. Williams, L.J.; Abdi, H. Fisher's Least Significant Difference (LSD) Test. In *Encyclopedia of Research Design*; Salkind, N., Ed.; Sage: Thousand Oaks, CA, USA, 2010; pp. 840–853.
67. Mendiburu, F. *Agricolae: Statistical Procedures for Agricultural Research, R Package Version 1.3-2*; R Core Team: Vienna, Austria, 2019; Volume 1.
68. Montgomery, D.; Peck, E.A.; Geoffrey, V. *Introduction to Linear Regression Analysis*, 5th ed.; John Wiley & Sons: Hoboken, NJ, USA, 2012.
69. Rawlings, J.O.; Pantula, S.G.; Dickey, D.A. *Applied Regression Analysis: A Research Tool*, 2nd ed.; Springer: New York, NY, USA, 1998.
70. Zuur, A.F.; Ieno, E.N.; Walker, N.J.; Saveliev, A.A.; Smith, G.M. *Mixed Effects Models and Extensions in Ecology with R*; Springer Science+Business Media: New York, NY, USA, 2009; Volume 574.
71. Durbin, J.; Watson, G.S. Testing for serial correlation in least squares regression. III. *Biometrika* **1971**, *58*, 1–19. [CrossRef]
72. Steinitz-Kannan, M. Comparative Limnology of Ecuadorian Lakes: A Study of Species Number and Composition of Plankton Communities of the Galapagos Islands and the Equatorial Andes. Ph.D. Thesis, Ohio State University, Columbus, OH, USA, 1979.
73. Miller, M.C.; Kannan, M.; Colinvaux, P.A. Limnology and primary productivity of Andean and Amazonian tropical lakes of Ecuador. *Int. Ver. Theor. Angew. Limnol. Verhandlungen* **1984**, *22*, 1264–1270. [CrossRef]
74. Gunkel, G. Limnology of an Equatorial High Mountain Lake in Ecuador, Lago San Pablo. *Limnologica* **2000**, *30*, 113–120. [CrossRef]
75. Gunkel, G.; Beulker, C. Limnology of the crater lake Cuicocha, Ecuador, a cold water tropical lake. *Int. Rev. Hydrobiol.* **2009**, *94*, 103–125. [CrossRef]
76. Van Colen, W.R.; Mosquera, P.; Vanderstukken, M.; Goiris, K.; Carrasco, M.C.; Decaestecker, E.; Alonso, M.; León-Tamariz, F.; Muylaert, K. Limnology and trophic status of glacial lakes in the tropical Andes (Cajas National Park, Ecuador). *Freshw. Biol.* **2017**, *62*, 458–473. [CrossRef]
77. Gómez-Giraldo, A.; Román-Botero, R.; Toro, F.M. Seasonal evolution of the thermal structure of a tropical reservoir. In Proceedings of the 16th Workshop on Physical Processes in Natural Waters, Queensland, Australia, 8–11 July 2013; pp. 2–3.
78. Zhang, Y.; Wu, Z.; Liu, M.; He, J.; Shi, K.; Zhou, Y.; Wang, M.; Liu, X. Dissolved oxygen stratification and response to thermal structure and long-term climate change in a large and deep subtropical reservoir (Lake Qiandaohu, China). *Water Res.* **2015**, *75*, 249–258. [CrossRef] [PubMed]
79. Lewis, W.M. Biogeochemistry of tropical lakes. *Int. Ver. Theor. Angew. Limnol. Verhandlungen* **2010**, *30*, 1595–1603. [CrossRef]
80. Posada-Bedoya, A.; Gómez-Giraldo, A.; Román-Botero, R. Effects of riverine inflows on the climatology of a tropical Andean reservoir. *Limnol. Oceanogr.* **2021**, *66*, 3535–3551. [CrossRef]
81. Román-Botero, R.; Gómez-Giraldo, A.; Toro-Botero, M. Efecto estacional de los afluentes en la estructura térmica de un pequeño embalse neotropical, La Fe—Colombia. *Dyna* **2013**, *80*, 152–161.
82. Hope, D.; Billett, M.F.; Cresser, M.S. A review of the export of carbon in river water: Fluxes and processes. *Environ. Pollut.* **1994**, *84*, 301–324. [CrossRef] [PubMed]
83. Tranvik, L.; Jansson, M. Climate change—Terrestrial export of organic carbon. *Nature* **2002**, *415*, 861–862. [CrossRef]
84. Thomas, S.; Cecchi, P.; Corbin, D.; Lemoalle, J. The different primary producers in a small African tropical reservoir during a drought: Temporal changes and interactions. *Freshw. Biol.* **2000**, *45*, 43–56. [CrossRef]
85. Gunkel, G.; Lange, U.; Walde, D.; Rosa, J.W.C. The environmental and operational impacts of Curuá-Una, a reservoir in the Amazon region of Pará, Brazil. *Lakes Reserv. Res. Manag.* **2003**, *8*, 201–216. [CrossRef]
86. Ministerio del Ambiente del Ecuador (MAE). *Sistema de Clasificación de Ecosistemas del Ecuador Continental*; Subsecretaría de Patrimonio Natural—Proyecto Mapa de Vegetación: Quito, Ecuador, 2013.
87. Salazar, R.N.; Aguirre, C.; Soto, J.; Salinas, P.; Salinas, C.; Prieto, H.; Paneque, M. Physicochemical parameters affecting the distribution and diversity of the water column microbial community in the high-altitude andean lake system of la brava and la punta. *Microorganisms* **2020**, *8*, 1181. [CrossRef]
88. Jones, B.E.; Grant, W.D.; Duckworth, A.W.; Owenson, G.G. Microbial diversity of soda lakes. *Extremophiles* **1998**, *2*, 191–200. [CrossRef]
89. Munawar, M. Limnological studies on freshwater ponds of Hyderabad—India. *Hydrobiologia* **1970**, *44*, 13–27. [CrossRef]

90. Hulyal, S.B.; Kaliwal, B.B. Dynamics of phytoplankton in relation to physico-chemical factors of Almatti reservoir of Bijapur District, Karnataka State. *Environ. Monit. Assess.* **2009**, *153*, 45–59. [CrossRef]
91. Lewis, W.M. Primary Production in the Plankton Community of a Tropical Lake. *Ecol. Monogr.* **1974**, *44*, 377–409. [CrossRef]
92. Kimmel, B.L.; Groeger, A.W. Factors controlling primary production in lakes and reservoirs: A perspective. *Lake Reserv. Manag.* **1984**, *1*, 277–281. [CrossRef]
93. Lee, Y.; Ha, S.Y.; Park, H.K.; Han, M.S.; Shin, K.H. Identification of key factors influencing primary productivity in two river-type reservoirs by using principal component regression analysis. *Environ. Monit. Assess.* **2015**, *187*, 213. [CrossRef] [PubMed]
94. Cartuche, A.; Guan, Z.; Ibelings, B.W.; Venail, P. Phytoplankton Diversity Relates Negatively with Productivity in Tropical High-Altitude Lakes from Southern Ecuador. *Sustainability* **2019**, *11*, 5235. [CrossRef]
95. Karlsson, J.; Jonsson, A.; Jansson, M. Productivity of high-latitude lakes: Climate effect inferred from altitude gradient. *Glob. Chang. Biol.* **2005**, *11*, 710–715. [CrossRef]
96. Feresin, E.G.; Arcifa, M.S.; da Silva, L.H.S.; Esguícero, A.L.H. Primary productivity of the phytoplankton in a tropical Brazilian shallow lake: Experiments in the lake and in mesocosms. *Acta Limnol. Bras.* **2010**, *22*, 384–396. [CrossRef]
97. Morin, A.; Lamoureux, W.; Busnarda, J. Empirical models predicting primary productivity from chlorophyll a and water temperature for stream periphyton and lake and ocean phytoplankton. *J. N. Am. Benthol. Soc.* **1999**, *18*, 299–307. [CrossRef]
98. Chattopadhyay, C.; Banerjee, T.C. Water Temperature and Primary Production in the Euphotic Zone of a Tropical Shallow Freshwater Lake. *Asian J. Exp. Sci* **2008**, *22*, 103–108.
99. Montecino, V. Primary productivity in South American temperate lakes and reservoirs. *Rev. Chil. Hist. Nat.* **1991**, *64*, 555–567.
100. Gunkel, G.; Casallas, J. Limnology of an equatorial high mountain lake—Lago San Pablo, Ecuador: The significance of deep diurnal mixing for lake productivity. *Limnologica* **2002**, *32*, 33–43. [CrossRef]
101. Herzog, S.K.; Martinez, R.; Jørgensen, P.M.; Tiesse, H. *Climate Change and Biodiversity in the Tropical Andes*; Inter-American Institute for Global Change Research (IAI): Montevideo, Uruguay; Scientific Committee on Problems of the Environment (SCOPE): Paris, France, 2011.

Disclaimer/Publisher's Note: The statements, opinions and data contained in all publications are solely those of the individual author(s) and contributor(s) and not of MDPI and/or the editor(s). MDPI and/or the editor(s) disclaim responsibility for any injury to people or property resulting from any ideas, methods, instructions or products referred to in the content.